Gypenosides attenuate retinal degeneration in a zebrafish retinitis pigmentosa model

Alhasani, Reem Hasaballah; Zhou, Xinzhi; Biswas, Lincoln; Li, Xing; Reilly, James; Zeng, Zhihong; Shu, Xinhua

Published in:
Experimental Eye Research

DOI:
10.1016/j.exer.2020.108291

Publication date:
2020

Document Version
Author accepted manuscript

Gypenosides attenuate retinal degeneration in a zebrafish retinitis pigmentosa model

Reem Hasaballah Alhasani[1,4], Xinzhi Zhou[1], Lincoln Biswas[1], Xing Li[5], James Reilly[1], Zhihong Zeng[2,*] and Xinhua Shu[1,3,5]*

[1]Department of Biological and Biomedical Sciences, Glasgow Caledonian University, Glasgow G4 0BA, United Kingdom

[2]College of Biological and Environmental Engineering, Changsha University, Changsha, Hunan 410022, P. R. China

[3]Department of Vision Science, Glasgow Caledonian University, Glasgow G4 0BA, United Kingdom

[4]Department of Biology, Faculty of Applied Science, Umm Al-Qura University, Makkah, Saudi Arabia

[5]School of Basic Medical Sciences, Shaoyang University, Shaoyang, Hunan 422000, P. R. China

* Corresponding authors: z20181201@ccsu.edu.cn; Xinhua.Shu@gcu.ac.uk

Abstract

Retinitis pigmentosa (RP) is a collection of heterogenous genetic retinal disorders resulting in cumulative retinal deterioration involving progressive loss of photoreceptors and eventually in total blindness. Oxidative stress plays a central role in this photoreceptor loss. Gypenosides (Gyp) are the main functional component isolated from the climbing vine *Gynostemma pentaphyllum* and have been shown to defend cells against the effects of oxidative stress and inflammation, providing protection in experimentally-induced optic neuritis. The zebrafish model has been used to investigate a range of human diseases. Previously we reported early retinal degeneration in a mutant zebrafish line carrying a point-nonsense mutation in the retinitis pigmentosa GTPase regulator interacting protein 1 (*rpgrip1)* gene that is mutated in RP patients. The current study investigated the potential protective effects of Gyp against photoreceptor degeneration in the Rpgrip1 deleted zebrafish. *Rpgrip1* mutant zebrafish were treated with 5µg/ml of Gyp in E3 medium from 6 hours post fertilization (hpf) till 1 month post fertilization (mpf). *Rpgrip1* mutant zebrafish treated with 5µg/mL of Gyp showed a significant decrease by 68.41% (p=0.0002) in photoreceptor cell death compared to that of untreated mutant zebrafish. Expression of antioxidant genes *catalase*, *sod1*, *sod2*, *gpx1*, *gclm*, *nqo-1* and *nrf-2* was significantly decreased in *rpgrip1* mutant zebrafish eyes by 61.51%, 77.40%, 60.11%, 81.17%, 72.07%, 78.95% and 85.42% (all p<0.0001), respectively, when compared to that of wildtype zebrafish; superoxide dismutase and catalase activities, and glutathione levels in *rpgrip1* mutant zebrafish eyes were significantly decreased by 87.21%, 21.55% and 96.51% (all p<0.0001), respectively. There were marked increases in the production of reactive oxygen species (ROS) and malondialdehyde (MDA) by

2738.73% and 510.69% (all p<0.0001), respectively, in *rpgrip1* mutant zebrafish eyes; expression of pro-inflammatory cytokines IL-1β, IL-6 and TNF-α was also significantly increased by 150.11%, 267.79% and 190.72% (all p<0.0001), respectively, in *rpgrip1* mutant zebrafish eyes, compared to that of wildtype zebrafish. Treatment with Gyp significantly counteracted these effects. This study indicates that Gyp has a potential role in the treatment of RP.

Keywords: Retinitis pigmentosa; RPGRIP1; photoreceptor death; zebrafish; Gypenosides

1. Introduction

Retinitis pigmentosa (RP, MIM# 268000) is the term applied to a diverse range of inherited retinal disorders characterised by initial death of rod photoreceptors followed by the death of cone photoreceptors. RP is one of the most common retinal dystrophies, affecting 1 in 3000-4000 people worldwide (Petra-Silva and Linden, 2014; Phelan and Bok, 2000; Raghupathy et al., 2013). Leber congenital amaurosis (LCA), the congenital version of RP, was first recognised and described by Leber (1869). LCA is perhaps the severest form of RP, affecting 1 in 40,000-80,000 worldwide and causing significant visual impairment within one year of birth (Sherwin et al., 2008; Stone, 2007). Characterisation of LCA is based on its clinical features: photophobia, sensory nystagmus, early severe visual loss, absent or reduced electroretinogram (ERG) waveform, and amaurotic pupils (Stone, 2007).

Mutations in the Retinitis Pigmentosa GTPase Regulator Interacting Protein 1 (*RPGRIP1*) gene cause LCA (LCA6) (Dryja et al., 2001; Gerber et al., 2001), juvenile RP (Booij et al., 2005), late onset cone-rod dystrophy (CORD13) in humans (Hameed et al., 2003; Huang et al., 2013; Khan et al., 2013) and cone-rod dystrophy in dogs (Mellersh et al., 2013). Around 5% of all LCA cases is thought to be caused by mutations in the *RPGRIP1* gene (Kumaran et al., 2017). Depletion of RPGRIP1 in human retinal pigment epithelial (RPE) cells causes cilia defects and abnormal cytoskeleton (Patnaik et al., 2018). Loss of RPGRIP1 in mice results in developmental defects in photoreceptor outer segments, mislocalization of rhodopsin, and early retinal degeneration (Won et al. 2009; Zhao et al., 2003). Recently we have characterized a mutant zebrafish line that carries a nonsense homozygous mutation in the *rpgrip1* gene. The mutant zebrafish demonstrate defects

91 in the development of the rod outer segment and in the trafficking of ciliary protein, early retinal
92 degeneration and impaired visual function (Raghupathy et al., 2017).

93 *Gynostemma pentaphyllum* (*G. pentaphyllum*) Makino (Jiaogulan in Chinese) is a
94 herbaceous vine plant – more accurately a kind of cucurbitaceous liana (gourd family with woody
95 vines to support its growth) – that is widely used in traditional medicine throughout Asia, including
96 the mountainous regions of Vietnam, Japan, Korea and China. *G. pentaphyllum* Makino contains a
97 variety of compounds including saponins, carotenoids, chlorophylls, flavonoids, polysaccharides,
98 sterols, amino acids, vitamins and minerals (Razmovski-Naumovski et al., 2005). Gypenosides
99 (Gyp), the dammarane-type saponins extract derived from the *G. pentaphyllum* (Thunb) Makino,
100 are yellow in colour and bitter tasting, and have anti-diabetic, anti-hyperlipedemic , anti-tumour,
101 anti-oxidative and anti-inflammatory properties (Li et al., 2019). We recently demonstrated that
102 Gyp protected RPE cells from H_2O_2-induced oxidative damage and inflammation (Alhasani et al.,
103 2018).

104 Current therapeutic strategies for RP include gene therapy, cell therapy, retinal prostheses
105 and pharmacological approaches (Dias et al., 2018). High genetic heterogeneity of RP and the
106 complexity of photoreceptor degeneration pathways make RP treatment extraordinarily
107 challenging. Oxidative stress has been implicated in the progression of RP. Treatment with
108 antioxidants has been shown to reduce oxidative damage and preserve photoreceptor function in
109 RP animal models (Komeima et al., 2006; Lee et al., 2011; Shen et al., 2005). There is a close link
110 between oxidative stress and inflammation. Mouse RP models exhibit increased proinflammatory
111 cytokines and chemokines preceding photoreceptor degeneration (Karlstetter et al., 2015; Yoshida

et al., 2013a; Xun et al., 2019). RP patients also have significantly higher levels of proinflammatory cytokines and chemokines in the vitreous fluid (Yoshida et al., 2013b). Microglial activation has been observed in the retinas of RP patients and RP rodent models and is associated with rod cell death (Gupta et al., 2003; Karlstetter et al., 2015; Zhao et al., 2015). Activated microglia phagocytose pre-apoptotic rod cells and secrete proinflammatory cytokines, which exacerbates rod death in RP mouse models; by contrast, inhibition of microglial activation attenuates rod cell death (Zhao et al., 2015). Antioxidants and anti-inflammatory agents offer a therapeutic option (Guadagni et al., 2015), and so there is a pressing need to identify novel anti-oxidative and anti-inflammation agents for the treatment of RP. In the current study we appraised the therapeutic potential of Gyp for RP by using it to treat *rpgrip1* mutant zebrafish and investigating subsequent biochemical and histological changes. We found that Gyp treatment delayed photoreceptor death, increased antioxidant capacity and inhibited endoplasmic reticulum (ER) stress and inflammation.

2. Materials and methods

2.1. Toxicity assay

All animal work received approval from the UK Home Office with Project licence PPL 70/8697. Gypenosides (Gyp), containing several gypenoside molecules, were purchased from Xi'an Jiatian Biotech Co. Ltd, China with 98% purity and dissolved in 100% Dimethyl sulfoxide (DMSO) as a stock (10 mg/mL). To determine the toxicity of Gyp in zebrafish embryonic stages, toxicity assay was carried out using previously described methods (Scholz et al., 2008). Zebrafish embryos at 6 hours post fertilization (hpf) were treated at 28 °C in twenty-four-well plates (10 embryos/well) containing 500 µl/well of Gyp at concentrations of 0, 2.5, 5.0, 15.0, 25.0 and 50.0 µg/ml in E3

medium (5 mM NaCl, 0.17 mM KCl, 0.33 mM CaCl2, 0.33 mM MgSO4). Mortality, heartbeat and hatching were recorded at 48, 72, 96 and 120 hpf. Heartbeat measurement was performed by putting individual embryos into E3 medium on a glass slide and visually counting ventricle beating (beats per minutes, BPM) under Evos microscope.

2.2. Zebrafish treatment

To investigate whether Gyp can inhibit or delay photoreceptor degeneration, *rpgrip1* mutant embryos at 6 hpf were treated with Gyp in E3 medium till one month post fertilization (mpf). There were 3 groups: wildtype in E3 medium (0.05 % DMSO), *rpgrip1* mutants in E3 medium (0.05 % DMSO), and *rpgrip1* mutants treated with Gyp (5 µg /mL in 0.05% DMSO). The treatment was carried out in 60mm×15mm petri dishes in which the sibling and *rpgrip1* mutant embryos (6 hpf) were incubated at 28°C in 4 mL E3 medium with or without Gyp (15 embryos/petri dish in triplicates). After 5 days, the embryos were transferred to 1-litre water tanks (15 fish/tank in 100 ml E3 medium) and kept at 24°C in the zebrafish facility for 25 days. During the treatment, fish were fed with ZM-100 fry food and brine shrimp (Zebrafish Management Ltd, UK). E3 medium (0.05 % DMSO) with or without Gyp (5µg /mL) was changed every two days. After the treatment, zebrafish were killed using Schedule one method and eyes were dissected for further examination.

2.3. Measurement of reactive oxygen species (ROS)

Eyes from wildtype, untreated and Gyp-treated *rpgrip1* mutant zebrafish at 1mpf were collected and homogenized using the FastPrep®-24 homogenizer (MP Biomedicals, UK) on ice in lysis buffer containing 1 mM MgCl2, 20 mM HEPES, 0.32 mM sucrose, and 0.5 mM phenylmethylsulfonyl fluoride (PMSF, pH 7.4). The lysates were centrifuged at 10,000Xg for 5 minutes at 4°C and the supernatants were treated with Dichloro-dihydro-fluorescein Diacetate (DCFH-DA) solution (20

156 µg/ml, 8.3 µl/well) in 96-well plates and incubated in darkness at 37°C for 30 min. The fluorescent
157 signal was measured using the Fluostar Optima microplate reader (BMG-labtech) at 485 nm
158 (excitation) and 525 nm (emission). The ROS level was calculated as previously described
159 (Alhasasni et al., 2018).

160 *2.4. Histology and immunohistochemistry (IHC)*

161 After one month of treatment, zebrafish eyes were dissected, fixed at 4°C for 24 hours in 4%
162 paraformaldehyde (PFA) solution, then washed with PBS twice, dehydrated with ethanol and
163 embedded in paraffin to make tissue wax blocks for histology; alternatively, the eyes were
164 incubated with 5%, 15% or 30% sucrose for 2 hours and then embedded in Optimal Cutting
165 Temperature (OCT) compound for cryosections. Eye samples of 8 µm thickness were sectioned by
166 microtome or cryotome. For histology, sections were dewaxed and stained with
167 haematoxylin-eosin. For measurement of the photoreceptor layer, five eyes from five individual
168 fish from each group were used, two retinal sections of each eye were selected and images were
169 taken from inferior sides. Thickness of the photoreceptor layer was measured using Image J
170 software at the location 0.4 mm from the optic nerve head. For IHC, cryosections were blocked for
171 30 minutes in 2% bovine serum albumin (BSA)/PBS and incubated with primary antibody
172 (anti-rhodopsin, Cat. ab98887, Abcam, 1:500 dilution) in 2% BSA/PBS at room temperature for 2
173 hours. The sections were washed three times (5 minutes/each) with PBS and then incubated with
174 secondary antibody (goat anti-mouse IgG FITC-conjugated, Cat. F0257, Sigma, UK (1:500 dilution)
175 in 2% BSA/PBS at room temperature for 1 hour. After washing with PBS five times (5
176 minutes/each), the sections were mounted with Vectashield 4',6-diamidino-2-phenylindole (DAPI)

(D9542-Sigma, UK). Images were taken with ZEISS LSM 800 confocal microscopy. To quantify the rhodopsin fluorescence signal, 10 retinal sections from five eyes (two sections/each eye) were collected from the control (wildtype zebrafish), *rpgrip1* mutants, or *rpgrip1* mutants treated with Gyp. In each section, one region (10 μm×10 μm, under ×400 magnification) in the superior side (0.4 mm from the optic nerve head) and one region (10 μm×10 μm, under ×400 magnification) in the inferior side (0.4 mm from the optic nerve head) were chosen for quantification of fluorescent signals with ImageJ software. The signals from both the superior region and the inferior region were averaged for the final calculation.

2.5. Gene expression

Total RNA was extracted from 20 eyes of wildtype, *rpgrip1* mutant, or Gyp-treated *rpgrip1* mutant zebrafish at 1 mpf by using the TRIzol reagent (Sigma, UK) according to the manufacturer's guidance. cDNA synthesis was performed using High-Capacity cDNA Reverse Transcription Kit (Applied Biosystems, UK). Quantitative real-time polymerase chain reaction (qRT-PCR) was carried out using Platinum® SYBR® Green QPCR SuperMix-UDG w/ROX kit (ThermoFisher Scientific, UK) following the manufacture's protocol. The primers for qRT-PCR are listed in Table S1. β-actin was used to normalize mRNA levels of candidate genes.

2.6. Measurement of activities of superoxide dismutase (SOD) and catalase (CAT) and quantification of glutathione (GSH) and malondialdehyde (MDA) levels

Activities of SOD and CAT and levels of GSH and MDA were measured in zebrafish eye samples using individual commercial kits (STA-340 for SOD, STA-341 for CAT, STA-312 for GSH and STA-330 for MDA from Cell Biolabs) following the manufacturer's instructions.

2.7. Western blotting

Twenty eyes from the groups of wildtype, *rpgrip1* mutant and Gyp-treated *rpgrip1* mutant zebrafish were homogenized in protein lysis buffer (T-PER, Thermo Fisher Scientific UK) using a FastPrep®-24 homogenizer (MP Biomedicals) on ice. Concentration of protein samples was measured by a Bradford assay. 100µg of individual protein samples was loaded in the pre-cast protein gel (Cat. No. 4569034, Bio-Rad) then electrophoresed for 45-60mins at 200V in the running buffer. The gel was removed from the electrophoresis apparatus and assembled into a sandwich containing three sponges, filter paper, pre-cast protein gel, nitrocellulose membrane, filter paper and three more sponges. The sponge-gel-membrane sandwich was then placed into a transfer cassette in the Wet Tank Transfer System (Cat. No. EI9051, Thermo Fisher Scientific) containing the transfer buffer to transfer the protein from the pre-cast protein gel onto the nitrocellulose membrane under 175mA for 90 minutes. The nitrocellulose membrane was blocked with Tris buffered saline with 0.1% Tween-20 (TBST) and 5% (w/v) non-fat dry milk for 2 hours at room temperature. The membrane was incubated with primary antibody (anti-acetylated tubulin antibody, Cat. T7451, Sigma, UK, 1:1000 dilution, anti-Caspase-3 antibody, Cat. ABIN1883652, Antibodies-online, UK, 1:1000 or anti-TNF-α antibody, Cat. ABIN1884227, Antibodies-online, UK, 1:1000 dilution) in TBST with 5% (w/v) non-fat dry milk for two hours. After washing three times with TBST, the membrane was incubated with secondary antibody (goat anti-rabbit antibody, Cat. 926–32211 or donkey anti-mouse antibody, Cat. 926–68072, 1:10,000 diluted in TBST with 5% non-fat dry milk) at room temperature for 2 hours. The membrane was washed five times (5 minutes/each). The band intensity of targeted proteins was measured using the LI-COR Odyssey FC Imaging System.

220 *2.8. Cell death detection*

221 Cell death in zebrafish eye sections was detected using DeadEnd™ fluorometric TUNEL assay
222 (Promega, UK) according to the manufacturer's instructions. Briefly, following dewaxation
223 zebrafish eye sections were treated with proteinase K solution (20 μg/ml), then incubated with
224 rTDT reaction at 37°C for one hour. The reaction was terminated with 2×SSC. The sections were
225 mounted with Vectashield DAPI (D9542-Sigma, UK) and the images were taken under ZEISS LSM
226 800 confocal microscopy. For quantification of cell death, six sections were chosen from six eyes
227 (one section/each eye) of control, *rpgrip1* mutant or Gyp-treated *rpgrip1* mutant group; in each
228 section, a region (50 μM×20 μM, long × wide) in the superior side (0.4 mm from the optic nerve
229 head) was chosen; TUNEL-positive photoreceptor cells in each region were counted and presented
230 as a percentage of the total number of photoreceptor cells in the same region.

231 *2.9. Statistical analysis*

232 Statistical analysis of the data was performed using GraphPad Prism 6 software via one-way
233 ANOVA (analysis of variance) followed by Bonferroni post hoc test. The data were calculated from
234 at least three independent experiments and shown as mean ± SEM (standard error of the mean). A
235 p value <0.05 was considered to be statistically significant.

236 **3. Results**

237 *3.1. Toxic effect of Gyp on zebrafish embryos and larvae*

238 Potential toxicity of Gyp was assessed to allow utilization of a safe dose for subsequent Gyp
239 treatment. Zebrafish embryos at 6 hpf were exposed to Gyp at different concentrations (2.5, 5, 15
240 and 25 μg/ml) for 5 days. Treatment with Gyp at 2.5 and 5 μg/ml resulted in mortality over this
241 period that was no different to that of the control group. Higher concentrations, however, caused

242 significantly increased mortality: 15 and 25 μg/ml Gyp resulted in, respectively, ~30% and ~60%
243 mortality at 120hpf (Figure S1A). The toxic effect of Gyp on cardiovascular development was
244 studied by monitoring the heart rate in control and treated groups at 72hpf. Only 25 μg/ml Gyp
245 treatment had a significant effect on heart rate compared to untreated controls. Heart rate in the
246 control group was typically ~100-120 beats/min; a similar rate was observed in zebrafish larvae
247 exposed to Gyp at 2.5, 5 or 15 μg/ml, whereas the 25 μg/ml Gyp-treated group showed a
248 significantly reduced heart rate of ~75 beats/min (Figure S1B). The hatching rate of zebrafish
249 embryos incubated with Gyp at different concentrations was also monitored at 72 hpf. The
250 hatching rate of 2.5 μg/ml and 5 μg/ml Gyp-treated embryos was 100%, identical to that of the
251 controls. However, zebrafish embryos treated with 15 or 25 μg/ml Gyp had a marked decrease in
252 hatching rate compared to the untreated control group (Figure S1C). Based on the above toxic
253 effects of Gyp on zebrafish embryos, we chose Gyp at 5 μg/mL for use in subsequent treatments.

254 *3.2. Gypenoside treatment rescued photoreceptor degeneration in rpgrip1 mutant zebrafish*

255 We have shown previously that outer / inner segments of *rpgrip1 mutant* zebrafish retina were
256 significantly shorter compared to the wildtype retina and that most rod cells had degenerated at
257 1mpf (Raghupathy et al., 2017). In the current study we performed retinal histology of wildtype,
258 Gyp-treated and untreated *rpgrip1 mutant* zebrafish at 1 mpf and confirmed that the
259 photoreceptor layer of *rpgrip1* mutants was significantly shorter compared to that of wildtype
260 zebrafish. The thickness of the wildtype photoreceptor layer was ~56 μm, while that of *rpgrip1*
261 mutant zebrafish was ~36μm. *Rpgrip1 mutant* zebrafish treated with 5μg/ml Gyp had a
262 significantly thickened photoreceptor layer of ~41μm, though the thickness of photoreceptor layer

in Gyp-treated *rpgrip1* mutant zebrafish was significantly less than that of wildtype zebrafish (Figure 1).

Rhodopsin has been shown to be mislocalized to the outer nuclear layer (ONL) of mouse *Rpgrip1* mutant retinas ((Won et al., 2009). Immunofluorescence staining of retinal sections with 4D2 antibody (detection of rhodopsin) revealed that only a weak signal of mislocalized rhodopsin was present in ONL of zebrafish *rpgrip1* mutant retinas, demonstrating early rod degeneration. Treatment of *rpgrip1 mutant* zebrafish with Gyp resulted in significantly increased signals of 4D2 staining (Figure 2A,B); when compared to wildtype, Gyp-treated zebrafish had significantly reduced 4D2 signals. *Rpgrip1* mutant zebrafish also had markedly lower mRNA level of *rhodopsin*, while Gyp treatment significantly increased *rhodopsin* mRNA level although still not as high as that seen in wildtype zebrafish (Figure 2C).

3.3. Gyp reduced photoreceptor cell death in rpgrip1 mutant zebrafish

Rpgrip1 mutant zebrafish have been shown to display significant cell death at examined time points: 14 days post fertilization (dpf), 1 mpf and 3 mpf (Raghupathy et al., 2017). In order to examine the protective role of Gyp, we carried out TUNEL assay to assess photoreceptor cell death. We observed significantly increased cell death in the ONL of the mutant zebrafish retinas, around 5-fold more compared to the control group. Gyp-exposed *rpgrip1* mutant embryos showed a marked decrease in photoreceptor cell death compared to that seen in untreated *rpgrip1* mutant zebrafish, while no difference was found between Gyp-treated and wildtype zebrafish (Figure 3).

We further examined whether the photoreceptor death was caspase-dependent by measuring the expression levels of caspase proteases, the key executioners of the apoptotic

process. Relative gene expression analysis using qRT-PCR showed significantly increased expression of *caspase3* in *rpgrip1* mutant zebrafish eyes compared to those of wildtype zebrafish. Gyp treatment resulted in significantly decreased expression of *caspase 3* gene in the mutant zebrafish (Figure S2A). Furthermore, we examined the protein level of Caspase 3 by Western blotting and found that Caspase 3 was significantly increased in rpgrip1 mutant eyes compared to that of wildtype zebrafish, while Gyp treatment significantly counteracted these changes (Figure S2B). When compared to wildtype zebrafish, Gyp-treated mutant zebrafish still had higher expression of Caspase 3 at mRNA and protein levels (Figure S2).

3.4. Gyp treatment can enhance the antioxidant capacity in *rpgrip1* mutant eyes

Excessive reactive oxygen species (ROS) production causes cell death through the oxidation and damage of macromolecules. We have shown previously that Gyp can suppress H_2O_2-induced ROS production in retinal epithelial cells (Alhasani et al., 2018). Therefore, we conjectured that excessive ROS production underlies increased photoreceptor cell death in *rpgrip1* mutant zebrafish retinas and that Gyp might reverse this effect. In fact, ROS production in *rpgrip1* mutant zebrafish eyes was 2766% higher than that in wildtype zebrafish. Treatment of mutant zebrafish with Gyp resulted in a significant decrease in ROS production by 63% compared to that of untreated *rpgrip1* mutant zebrafish eyes; however, even when treated with Gyp, mutant zebrafish had a higher production of ROS than did wildtype zebrafish (Figure 4A).

We then assessed the effect of Gyp on antioxidant gene expression using qRT-PCR. We observed that expression of *catalase*, *sod1*, sod2, *glutathione peroxidase 1* (*gpx1*), glutamate-cysteine ligase modifier subunit *(gclm)*, NAD(P)H quinone oxidoreductase-1 (*nqo1*) and

NF-E2-related factor-2 (*nrf2*) genes were markedly decreased in the mutant zebrafish eyes when compared to that of wildtype zebrafish. Gyp exposure significantly increased the expression of the examined antioxidant genes compared to that of untreated *rpgrip1* mutant zebrafish. When compared to wildtype zebrafish, Gyp-treated zebrafish had, with the exception of sod2, a lower expression of the examined genes (Figure 4B-H).

We also measured SOD and catalase activities and the levels of glutathione (GSH) and malondialdehyde (MDA) in the eyes of wildtype, untreated and Gyp-treated *rpgrip1* mutant zebrafish. SOD and catalase activities in *rpgrip1* mutant zebrafish eyes were significantly decreased when compared to that of wildtype zebrafish; Gyp treatment significantly increased SOD and catalase activities compared to that of untreated *rpgrip1* mutant zebrafish, though activities of both enzymes were still lower than that in wildtype zebrafish (Figure 5A, B). GSH level was significantly lower in *rpgrip1* mutant zebrafish eyes compared to that of wildtype zebrafish; treatment with Gyp significantly increased GSH level compared to that of untreated *rpgrip1* mutant zebrafish; when compared to wildtype zebrafish, Gyp-treated zebrafish eyes had a lower level of GSH (Figure 5C). The level of MDA was higher in *rpgrip1* mutant zebrafish eyes compared to wildtype zebrafish, while Gyp treatment resulted in a significantly decreased MDA level compared to that of untreated *rpgrip1* mutant zebrafish; compared to wildtype zebrafish, MDA level in Gyp-treated mutant zebrafish eyes was higher (Figure 5D).

3.5. Protective effect of Gypenoside against ER stress

ROS production and ER stress are closely related events. ER stress leads to increased transcription and translational responses, thereby causing an increased expression of ER stress inducers (Hetz et

al., 2011). Accordingly, we examined expression of *xbp1t* (total) and its spliced variant *xbp1s*, *atf4*, *atf6* and *bip*, all of which are induced in ER stress. Expression of all these genes was significantly higher in *rpgrip1* mutant zebrafish eyes compared to wildtype zebrafish, while expression was significantly lower in *rpgrip1* mutant zebrafish eyes that were treated with Gyp compared to those that were untreated. Expression of *atf6*, *xbp1s* and *xbp1t* (but not *atf4* or *bip*) remained significantly higher in mutant zebrafish treated with Gyp compared to that of wildtype zebrafish (Figure 6).

3.6. Gyp inhibited inflammation in rpgrip1 mutant zebrafish

We also examined expression of proinflammatory cytokines (*il-1β*, *il-6* and *tnf-α*) using qRT-PCR and found that expression of these genes was significantly higher in *rpgrip1* mutant zebrafish eyes compared to that of wildtype zebrafish; Gyp treatment significantly reduced expression of the three cytokines (Figure 7A). The change of Tnf-α protein level in Gyp-treated *rpgrip1* mutant was also confirmed by Western blotting. Expression of the proinflammatory cytokines was higher in Gyp-treated zebrafish eyes compared with that of wildtype zebrafish eyes (Figure 7B).

4. Discussion

The morphological and functional retinal cell impairment observed in RP is often a result of molecular changes triggered by the retinal damage (Dias et al. 2018). This retinal degeneration might be prompted by several factors including genetic predispositions, higher intraocular pressure, increased blood glucose levels, oxidative/nitrosative stress, or even aging. Irrespective of the trigger factor, a subsequent cascade of cell signals leads to well-established morphological and functional modifications such as apoptosis and retinal remodelling (Dias et al. 2018). Moreover,

oxidative stress, inflammatory response and induction of apoptotic pathways are characteristic traits in RP (Guadagni et al. 2015).

As a result of the high metabolic activity of photoreceptors, which have the greatest oxygen consumption rate per gram of any body tissue (Ames III, 1992), oxidative stress contributes significantly to the progression of RP (Komeima et al., 2006; Shen et al., 2005; Usui et al., 2009). Numerous animal models of RP suggest that ROS is a stimulus that triggers apoptotic photoreceptor cell death in RP and is aggravated by oxidative stress (Cuenca et al., 2014). Several studies have suggested that the secondary loss of cone cells that is characteristic of RP is a result of damage arising from the higher oxygen consumption and subsequent increased ROS levels when rod cells die (Carmody and Cotter, 2000; Shen et al., 2005). Moreover, ROS production due to light exposure has been demonstrated to exacerbate retinal degeneration in hereditary and age-linked retinopathies including RP (Paskowitz et al., 2006; Sui et al., 2013).

Previous studies have demonstrated that Gyp enhance antioxidant capacity, inhibit inflammation and suppress apoptotic cell death in *in vivo* animal models, such as ischemia/reperfusion injury rodent models (Ye et al., 2016; Yu et al., 2016a; Yu et al. 2016b;, Yu et al., 2016c; Zhao et al., 2014). More recently, Gyp have been shown to exhibit protective effects in rodent optic neuritis models by inhibiting lipopolysaccharide (LPS) or myelin oligodendrocyte glycoprotein (MOG) 35-55 peptide-induced inflammation (Wang et al., 2018; Zhang et al., 2017). There are few studies, however, on its role in retinal degeneration. Our previous *in vitro* study demonstrated that Gyp suppress ROS generation in the ARPE-19 cell line via its effects on gene expression and protein level of several antioxidant scavengers and apoptosis-related genes

(Alhasani et al., 2018). Our current research has shown that *rpgrip1* mutant zebrafish had significantly higher production of ROS and MDA, lower expression of antioxidant genes, less GSH and high level of rod cell death; Gyp treatment significantly reduced generation of ROS and MDA and increased antioxidant gene expression and GSH level, arresting rod cell degeneration.

The NRF2 pathway plays an important role in cellular defence against oxidative damages (Lim et al., 2014). NRF2 is involved in the regulation of several cellular defence mechanisms that counteract the potentially lethal consequences of ROS (Lim et al., 2014). In stress-free conditions NRF2 is localized to the cytoplasm but in the presence of oxidative stress is phosphorylated and translocated to the nucleus, in turn activating several cytoprotective genes (Lim et al., 2014). Activation of the NRF2 functional pathway has been reported to protect against photoreceptor degeneration in RP animal models. Nakagami et al. (2016) demonstrated that NRF2 activation and upregulation of its effector proteins slowed photoreceptor cell death in a RP rabbit model. Adeno-associated virus (AAV)-mediated overexpression of NRF2 in the retina alleviated photoreceptor degeneration in three RP mouse models (Xiong et al., 2015). We too found that *rpgrip1* mutant zebrafish eyes had lower expression of NRF2 and its targeting antioxidant genes and that Gyp treatment increased expression of these genes, suggesting that Gyp protection is possibly mediated by the NRF2 signalling pathway.

Impairment of protein folding and maturation in ER causes ER stress, leading to the unfolded protein response (UPR). UPR is mediated by protein kinase RNA-like endoplasmic reticulum kinase (PERK), inositol-requiring enzyme 1 (IRE1) and activating transcription factor 6 (ATF6) signalling pathways. ER stress has been implicated in the pathogenesis of RP, while pharmacological

389 inhibition of ER stress has been shown to slow retinal degeneration in RP animal models (Dias et
390 al., 2018; Zhang et al., 2014). Previous studies demonstrated that Gyp protected cardiomyocytes
391 from ischemia-reperfusion injury-induced apoptosis via inactivation of C/EBP homologous
392 protein-10 (CHOP) (Yu et al., 2016c). Here we showed that *rpgrip1* mutant eyes had higher
393 expression of *atf4*, *atf6*, *xbp1* and *bip* genes, which encode proteins involved in the UPR. Gyp
394 treatment led to significantly decreased expression of these genes, suggesting that Gyp inhibited
395 ER stress that may contribute to decreased rod apoptosis in Gyp-treated *rpgrip1* mutant zebrafish.
396 Inflammatory cytokines are overproduced upon exposure to ROS/oxidative stress. Several
397 studies have reported the secretion of various proinflammatory cytokines and chemokines into
398 the vitreous cavity in RP and other ocular diseases, with these cytokines and chemokines being
399 partly responsible for the initiation and development of the condition (Funatsu et al., 2005;
400 Yoshida et al., 2013a; Yoshida et al., 2013b; Yoshimura et al., 2009). Our previous study
401 demonstrated that deletion of RPGR, an RPGRIP1 interaction protein, caused microglial activation
402 and higher IL-1β expression in mouse retinas (Zhang et al., 2019). In the current study, we also
403 found higher expression of proinflammatory cytokines (il-1β, il-6 and tnf-α) in *rpgrip1* mutant eyes
404 and showed that Gyp significantly decreased expression of these genes.
405 In conclusion, we observed that loss of Rpgrip1 in zebrafish resulted in a defective
406 antioxidant defense system and increased ER stress and inflammation. Gyp treatment inhibited
407 oxidative damage, ER stress and inflammation, resulting in slowdown of photoreceptor death in
408 *rpgrip1* mutant zebrafish.

Acknowledgments This study was funded by a Saudi Arabia government PhD scholarship, the Rosetrees Trust, National Eye Research Centre and the Lotus Scholarship Program of Hunan Province, China. X.S. is a Visiting Professor to Shaoyang University.

References

Alhasani, R.H., Biswas, L., Tohari, A.M., Zhou, X., Reilly, J., He, J.F., Shu, X., 2018. Gypenosides protect retinal pigment epithelium cells from oxidative stress. Food Chem. Toxicol. 112, 76-85.

Ames III, A., 1992. Energy requirements of CNS cells as related to their function and to their vulnerability to ischemia: a commentary based on studies on retina. Can. J. Physiol. Pharmacol. 70 Suppl, S158-S164.

Booij, J.C., Florijn, R.J., ten Brink, J.B., Loves, W., Meire, F., van Schooneveld, M.J., de Jong, P.T., Bergen, A.A., 2005. Identification of mutations in the AIPL1, CRB1, GUCY2D, RPE65, and RPGRIP1 genes in patients with juvenile retinitis pigmentosa. J. Med. Genet. 42, e67.

Carmody, R.J., Cotter, T.G., 2000. Oxidative stress induces caspase-independent retinal apoptosis in vitro. *Cell Death Differ*. 7, 282-291.

Cuenca, N., Fernández-Sánchez, L., Campello, L., Maneu, V., De la Villa, P., Lax, P., Pinilla, I., 2014. Cellular responses following retinal injuries and therapeutic approaches for neurodegenerative diseases. Prog. Retin. Eye Res. 43, 17-75.

Dias, M.F., Joo, K., Kemp, J.A., Fialho, S.L., da Silva Cunha, A. Jr., Woo, S.J., Kwon, Y.J., 2018. Molecular genetics and emerging therapies for retinitis pigmentosa: Basic research and clinical perspectives. Prog. Retin. Eye Res. 63, 107-131.

Dryja, T.P., Adams, S.M., Grimsby, J.L., McGee, T.L., Hong, D.H., Li, T., Andréasson, S., Berson, E.L., 2001. Null RPGRIP1 alleles in patients with Leber congenital amaurosis. Am. J. Hum. Genet. 68, 1295-1298.

Funatsu, H., Yamashita, H., Noma, H., Mimura, T., Nakamura, S., Sakata, K., Hori, S., 2005. Aqueous humor levels of cytokines are related to vitreous levels and progression of diabetic retinopathy in diabetic patients. Graefes Arch. Clin. Exp. Ophthalmol. 243, 3-8.

Gerber, S., Perrault, I., Hanein, S., Barbet, F., Ducroq, D., Ghazi, I., Martin-Coignard, D., Leowski, C., Homfray, T., Dufier, J.L., 2001. Complete exon-intron structure of the RPGR-interacting protein (RPGRIP1) gene allows the identification of mutations underlying Leber congenital amaurosis. Eur. J. Hum. Genet. 9, 561–571.

Guadagni, V., Novelli, E., Piano, I., Gargini, C., Strettoi, E., 2015. Pharmacological approaches to retinitis pigmentosa: A laboratory perspective. Prog. Retin. Eye Res. 48, 62-81.

Gupta, N., Brown, K.E., Milam, A.H., 2003. Activated microglia in human retinitis pigmentosa, late-onset retinal degeneration, and age-related macular degeneration. Exp. Eye Res., *76,* 463-471.

Hameed, A., Abid, A., Aziz, A., Ismail, M., Mehdi, S.Q., Khaliq, S., 2003. Evidence of RPGRIP1 gene mutations associated with recessive cone-rod dystrophy. J. Med. Genet. 40, 616– 619.

Hetz, C., Martinon, F., Rodriguez, D., Glimcher, L.H., 2011. The unfolded protein response: integrating stress signals through the stress sensor IRE1α. Physiol. Rev. 91, 1219-1243.

Huang, L., Zhang, Q., Li, S., Guan, L., Xiao, X., Zhang, J., Jia, X., Sun, W., Zhu, Z., Gao, Y., 2013. Exome sequencing of 47 chinese families with cone-rod dystrophy: mutations in 25 known causative genes. PloS One. 8, e65546.

Karlstetter, M., Scholz, R., Rutar, M., Wong, W. T., Provis, J. M., & Langmann, T., 2015. Retinal microglia: Just bystander or target for therapy? Prog. Retin. Eye Res, 45, 30–57.

Khan, A.O., Abu-Safieh, L., Eisenberger, T., Bolz, H.J., Alkuraya, F.S., 2013. The RPGRIP1-related retinal phenotype in children. Br. J. Ophthalmol. 97, 760-764.

Komeima, K., Rogers, B.S., Lu, L., Campochiaro, P.A., 2006. Antioxidants reduce cone cell death in a model of retinitis pigmentosa. Proc. Natl. Acad. Sci. U S A. 103, 11300-11305.

Kumaran, N., Moore, A.T., Weleber, R.G., Michaelides, M., 2017. Leber congenital amaurosis/early-onset severe retinal dystrophy: clinical features, molecular genetics and therapeutic interventions. Br. J. Ophthalmol. 101, 1147-1154.

Leber, T., 1869. Uber retinitis pigmentosa und angeborene amaurose. Graefes Arch. Clin. Exp. Ophthalmol. 15, 1-25.

Li, K., Ma, C., Li, H., Dev, S., He, J., Qu, X., 2019. Medicinal Value and Potential Therapeutic Mechanisms of Gynostemma pentaphyllum (Thunb.) Makino and Its Derivatives: An Overview. Curr. Top. Med. Chem. 19, 2855-2867.

Lim, J.L., Wilhelmus, M.M., de Vries, H.E., Drukarch, B., Hoozemans, J.J., van Horssen, J., 2014. Antioxidative defense mechanisms controlled by Nrf2: state-of the-art and clinical perspectives in neurodegenerative diseases. Arch. Toxicol. 88, 1773-1786.

Mellersh, C.S., Boursnell, M.E.G., Pettitt, L., Ryder, E.J., Holmes, N.G., Grafham, D., Forman, O.P., Sampson, J., Barnett, K.C., Blanton, S., 2006. Canine RPGRIP1 mutation establishes cone – rod dystrophy in miniature longhaired dachshunds as a homologue of human Leber congenital amaurosis. Genomics 88, 293–301.

471 Nakagami, Y., Hatano, E., Inoue, T., Yoshida, K., Kondo, M., Terasaki, H., 2016. Cytoprotective
472 effects of a novel Nrf2 activator, RS9, in rhodopsin Pro347Leu rabbits. Curr. Eye Res. 41,
473 1123-1126.
474 Paskowitz, D.M., LaVail, M.M., Duncan, J.L., 2006. Light and inherited retinal degeneration. Br. J.
475 Ophthalmol. 90, 1060-1066.
476 Patnaik, S.R., Zhang, X., Biswas, L., Akhtar, S., Zhou, X., Kusuluri, D.K., Reilly, J., MaySimera, H.,
477 Chalmers, S., McCarron, J.G., Shu, X., 2018. RPGR protein complex regulates proteasome activity
478 and mediates store-operated calcium entry. Oncotarget 9, 23183-23197.
479 Petrs-Silva, H., Linden, R., 2014. Advances in gene therapy technologies to treat retinitis
480 pigmentosa. Clin. Ophthalmol. 8, 127-136.
481 Phelan, J.K.; Bok, D., 2000. A brief review of retinitis pigmentosa and the identified retinitis
482 pigmentosa genes. Mol. Vis. 6, 116–124.
483 Raghupathy, R.K., McCulloch, D.L., Akhtar, S., Al-mubrad, T.M., Shu, X., 2013. Zebrafish model for
484 the genetic basis of X-linked retinitis pigmentosa. Zebrafish 10, 62–69.
485 Raghupathy, R.K., Zhang, X., Liu, L., Alhasani, R.H., Biswas, L., Akhtar, S., Pan, L., Moens, C.B., Li, W.,
486 Liu, M., Kennedy, B.N., Shu, X., 2017. Rpgrip1 is required for rod outer segment development and
487 ciliary protein trafficking in zebrafish. Sci. Rep. 7, 16881.
488 Razmovski-Naumovski, V., Huang, T.H.W., Tran, V.H., Li, G.Q., Duke, C.C., Roufogalis, B.D., 2005.
489 Chemistry and pharmacology of Gynostemma pentaphyllum. Phytochem. Rev. 4, 197-219.

490 Scholz, S., Fischer, S., Gündel, U., Küster, E., Luckenbach, T., Voelker, D., 2008. The zebrafish
491 embryo model in environmental risk assessment—applications beyond acute toxicity testing.
492 Environ. Sci. Pollut. Res. Int. 15, 394-404.
493 Shen, J., Yang, X., Dong, A., Petters, R.M., Peng, Y.W., Wong, F., Campochiaro, P.A., 2005. Oxidative
494 damage is a potential cause of cone cell death in retinitis pigmentosa. J. Cell. Physiol. 203,
495 457-464.
496 Sherwin, J.C., Hewitt, A.W., Ruddle, J.B., Mackey, D.A., 2008. Genetic isolates in ophthalmic
497 diseases. Ophthalmic Genet. 29, 149-161.
498 Stone, E. M., 2007. Leber congenital amaurosis - a model for efficient genetic testing of
499 heterogeneous disorders: LXIV Edward Jackson Memorial Lecture. Am. J. Ophthalmol. 144,
500 791-811.
501 Sui, G.Y., Liu, G.C., Liu, G.Y., Gao, Y.Y., Deng, Y., Wang, W.Y., Tong, S.H., Wang, L., 2013. Is sunlight
502 exposure a risk factor for age-related macular degeneration? A systematic review and
503 meta-analysis. Br. J. Ophthalmol. 97, 389-394.
504 Usui, S., Komeima, K., Lee, S.Y., Jo, Y.J., Ueno, S., Rogers, B.S., Wu, Z., Shen, J., Lu, L., Oveson, B.C.,
505 2009. Increased expression of catalase and superoxide dismutase 2 reduces cone cell death in
506 retinitis pigmentosa. Mol. Ther. 17, 778-786.
507 Wang, F., Dang, Y., Wang, J., Zhou, T., Zhu, Y., 2018. Gypenosides attenuate
508 lipopolysaccharide-induced optic neuritis in rats. *Acta Histochem*. 120, 340-346.

509 Won, J., Gifford, E., Smith, R.S., Yi, H., Ferreira, P.A., Hicks, W.L., Li, T., Naggert, J.K., Nishina, P.M.,
510 2009. RPGRIP1 is essential for normal rod photoreceptor outer segment elaboration and
511 morphogenesis. Hum. Mol. Genet. 18, 4329-4339.
512 Xiong, W., Garfinkel, A.E.M., Li, Y., Benowitz, L.I., Cepko, C.L., 2015. NRF2 promotes neuronal
513 survival in neurodegeneration and acute nerve damage. J. Clin. Invest. *125*, 1433-1445.
514 Ye, Q., Zhu, Y.I., Ye, S., Liu, H., She, X., Niu, Y., Ming, Y., 2016. Gypenoside attenuates renal
515 ischemia/reperfusion injury in mice by inhibition of ERK signaling. Exp. Ther. Med. 11, 1499–1505.
516 Yoshida, N., Ikeda, Y., Notomi, S., Ishikawa, K., Murakami, Y., Hisatomi, T., Enaida, H., Ishibashi, T.,
517 2013a. Laboratory evidence of sustained chronic inflammatory reaction in retinitis pigmentosa.
518 Ophthalmology 120, e5-12.
519 Yoshida, N., Ikeda, Y., Notomi, S., Ishikawa, K., Murakami, Y., Hisatomi, T., Enaida, H., Ishibashi, T.,
520 2013b. Clinical evidence of sustained chronic inflammatory reaction in retinitis pigmentosa.
521 Ophthalmology 120, 100-105.
522 Yoshimura, T., Sonoda, K.H., Sugahara, M., Mochizuki, Y., Enaida, H., Oshima, Y., Ueno, A., Hata, Y.,
523 Yoshida, H., Ishibashi, T., 2009. Comprehensive analysis of inflammatory immune mediators in
524 vitreoretinal diseases. PLoS One 4, e8158.
525 Yu, H., Guan, Q., Guo, L., Zhang, H., Pang, X., Cheng, Y., Zhang, X., Sun, Y., 2016a. Gypenosides
526 alleviate myocardial ischemia-reperfusion injury via attenuation of oxidative stress and
527 preservation of mitochondrial function in rat heart. Cell Stress Chaperones 21, 429–437.
528 Yu, H., Shi, L., Qi, G., Zhao, S., Gao, Y, Li, Y., 2016b. Gypenoside protects cardiomyocytes
529 against ischemia-reperfusion injury via the inhibition of mitogen-activated protein kinase
530 mediated nuclear factor kappa B pathway in vitro and in vivo. Front. Pharmacol. 7, 148.

Yu, H., Zhang, H., Zhao, W., Guo, L., Li, X., Li, Y., Zhang, X., Sun, Y., 2016c. Gypenoside protects against myocardial ischemia-reperfusion injury by inhibiting cardiomyocytes apoptosis via inhibition of CHOP pathway and activation of PI3K/Akt pathway in vivo and in vitro. Cell. Physiol. Biochem. 39, 123–136.

Zhang X., Shahani U., Reilly J., Shu X., 2019. Disease mechanisms and neuroprotection by tauroursodeoxycholic acid in Rpgr knockout mice. J. Cell. Physiol. 234, 18801-18812.

Zhang, H.K., Ye, Y., Zhao, Z.N., Li, K.J., Du, Y., Hu, Q.M., He, J.F., 2017. Neuroprotective effects of gypenosides in experimental autoimmune optic neuritis. *Int. J. Ophthalmol.* 10, 541-549.

Zhang, S.X., Sanders, E., Fliesler, S.J. and Wang, J.J., 2014. Endoplasmic reticulum stress and the unfolded protein responses in retinal degeneration. Exp. Eye Res. 125, 30-40.

Zhao, J., Ming, Y., Wan, Q., Ye, S., Xie, S., Zhu, Y., Wang, Y., Zhong, Z., Li, L., Ye, Q., 2014. Gypenoside attenuates hepatic ischemia/reperfusion injury in mice via antioxidative and anti-apoptotic bioactivities. Exp. Ther. Med. 7, 1388–1392.

Zhao, L., Zabel, M.K., Wang, X., Ma, W., Shah, P., Fariss, R.N., Qian H, Parkhurst, C.N., Gan, W.B., Wong, W.T., 2015. Microglial phagocytosis of living photoreceptors contributes to inherited retinal degeneration. EMBO Mol. Med. 7, 1179–1197.

Zhao, Y., Hong, D.H., Pawlyk, B., Yue, G., Adamian, M., Grynberg, M., Godzik, A. and Li, T., 2003. The retinitis pigmentosa GTPase regulator (RPGR)-interacting protein: subserving RPGR function and participating in disk morphogenesis. Proc. Natl. Acad. Sci. U S A, 100, 3965-3970.

Figures and legends

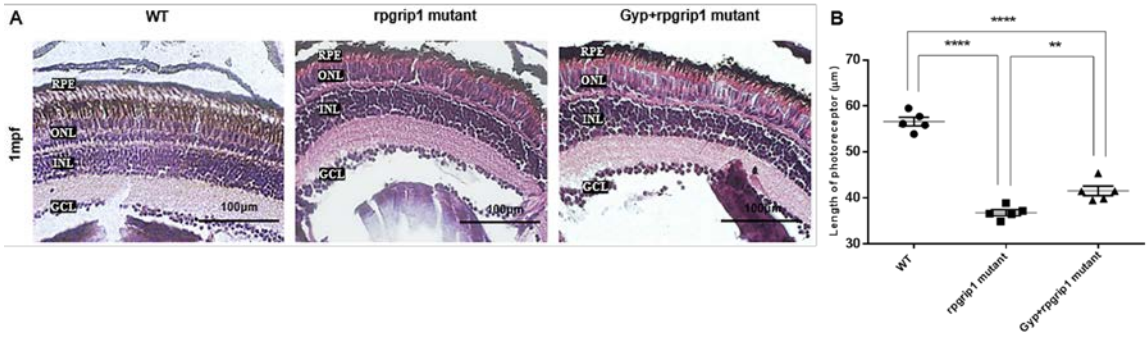

Figure 1 (A) Representative image of hematoxylin and eosin stained transverse retinal sections of wildtype (WT), untreated (UT) *rpgrip1* mutant and Gyp-treated *rpgrip1* mutant zebrafish at 1 mph. (B) Quantification of the length of photoreceptor cell layer of the examined zebrafish. GCL, ganglion cell layer; INL, inner nuclear layer; ONL, outer nuclear layer; RPE, retinal pigment epithelial cells. The data were analysed using one-way ANOVA followed by appropriate post hoc test (Bonferroni) and presented as mean ± SEM. $^{**}p < 0.01$ and $^{****}p < 0.0001$.

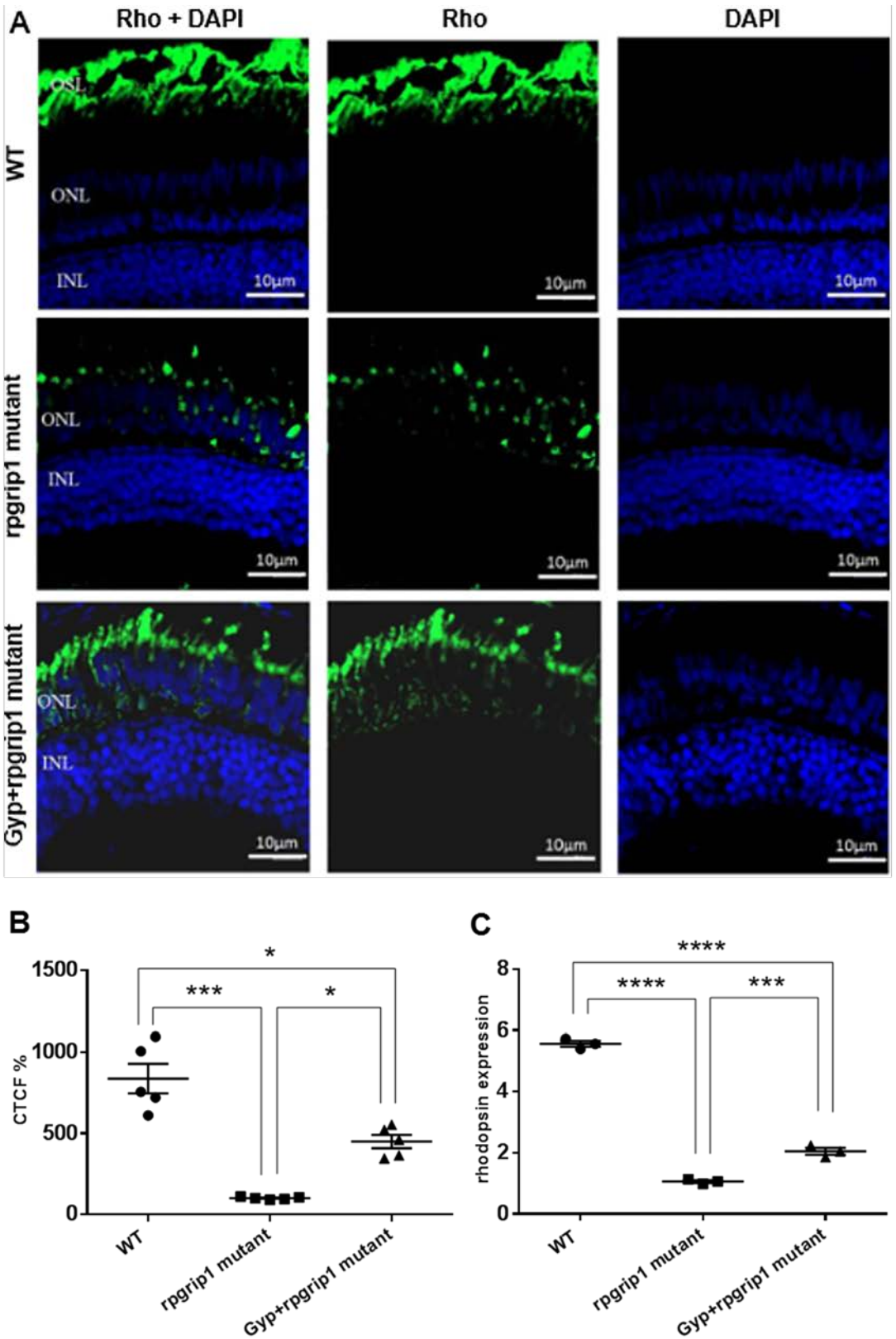

570

571 **Figure 2** (A) Immunostaining of transverse retinal sections of wildtype (WT), untreated

572 (UT) and Gyp-treated *rpgrip1* mutant zebrafish at 1mpf using 4D2 antibody. Rhodopsin

573 localization in the rods was visualized by green fluorescent signals, while nuclei were

574 labelled in blue by staining with DAPI. (B) Quantification of the corrected total cell
575 fluorescence (CTCF %) of rods in retinal sections of examined zebrafish. (C) Expression of
576 *rhodopsin* was examined by qRT-PCR. INL, inner nuclear layer; ONL, outer nuclear layer.
577 All data were analysed using one-way ANOVA followed by appropriate post hoc test
578 (Bonferroni) and presented as mean ± SEM. *$p < 0.05$, ***$p < 0.001$, ****$p < 0.0001$.
579
580
581
582
583
584
585
586
587
588
589
590

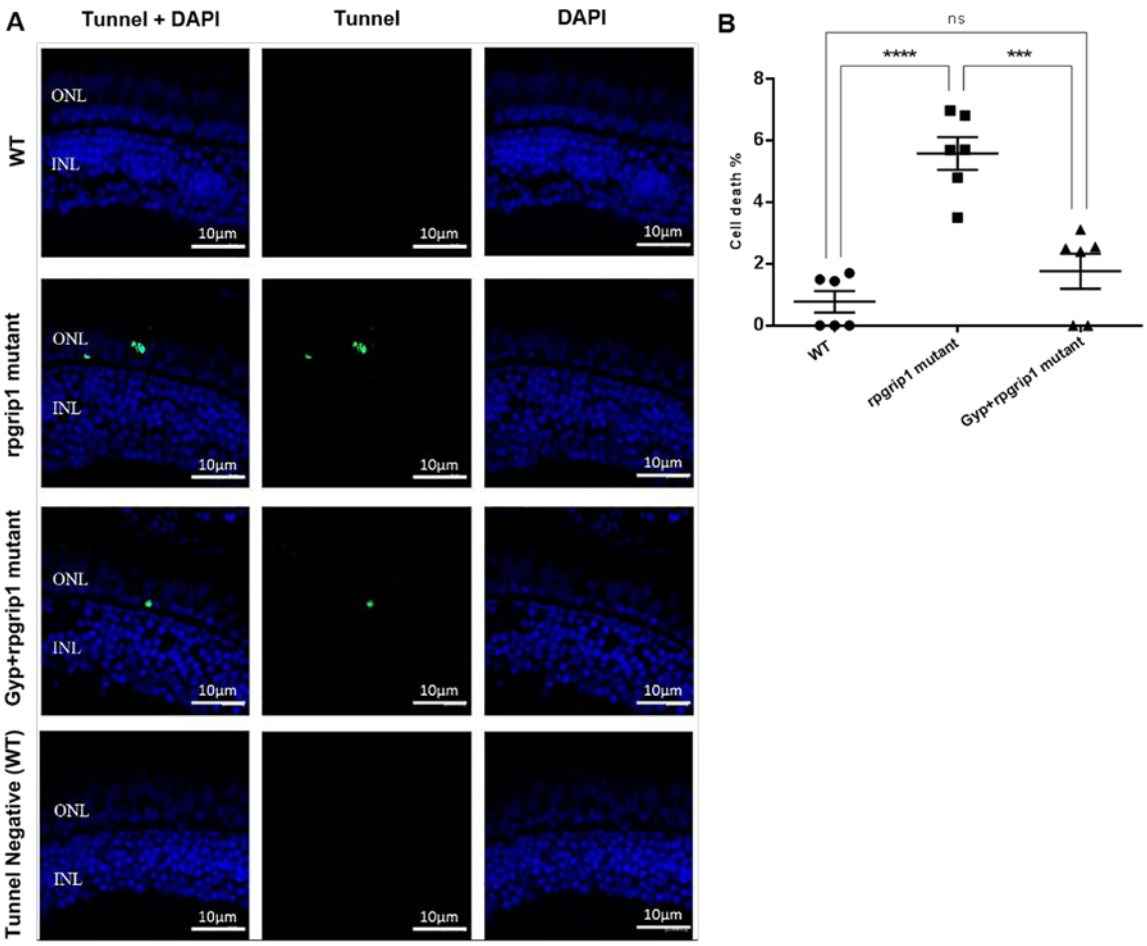

591

592 **Figure 3** (A) Photoreceptor cell death in wildtype (WT), untreated (UT) and Gyp-treated *rpgrip1*
593 mutant zebrafish at 1 mpf retinas was detected using TUNEL assay and photographed by ZEISS
594 LSM 800. (B) The number of cells labelled with positive TUNEL signal was counted within a 50
595 μm x 20μm (long×wide) area in the outer nuclear layer of the retinal section. The averaged
596 percentage of cells with positive TUNEL signal was counted from six individual animals from
597 each group. A negative control was set up using retinal sections from wildtype zebrafish at 1 mpf
598 incubated with the buffer without rTDT. INL, inner nuclear layer; ONL, outer nuclear layer. Data of
599 the fluorescent cells counting were analysed using one-way ANOVA followed by appropriate post
600 hoc test (Bonferroni) and presented as mean ± SEM. ns, no significance. ***$P < 0.001$ and ****$P <$
601 0.0001.

602

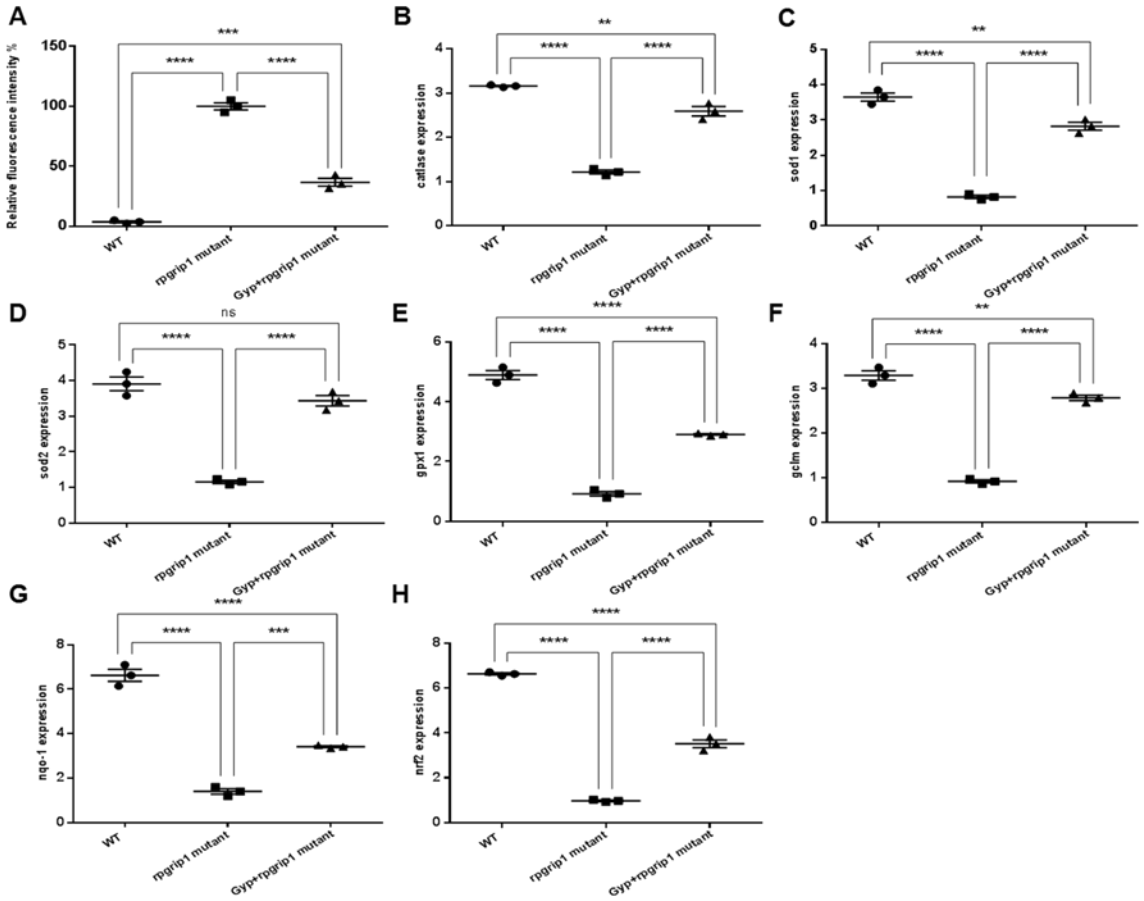

Figure 4. (A) ROS production in eye samples of wildtype (WT), untreated (UT) or Gyp-treated *rpgrip1* mutant zebrafish at 1 mpf was measured using DCFH-DA staining described in Materials and methods section. (B-H) Expression of antioxidant genes *catalase*, *sod1*, *sod2*, *gpx1*, *gclm*, *nqo-1* and *nrf2* in the eye samples of wildtype (WT), untreated (UT) or Gyp-treated *rpgrip1* mutant zebrafish at 1 mpf was measured by qRT-PCR. All data were analysed using one-way ANOVA followed by appropriate post hoc test (Bonferroni) and presented as mean ± SEM. *$p < 0.05$, **$p < 0.01$, ***$p < 0.001$ and ****$p < 0.0001$.

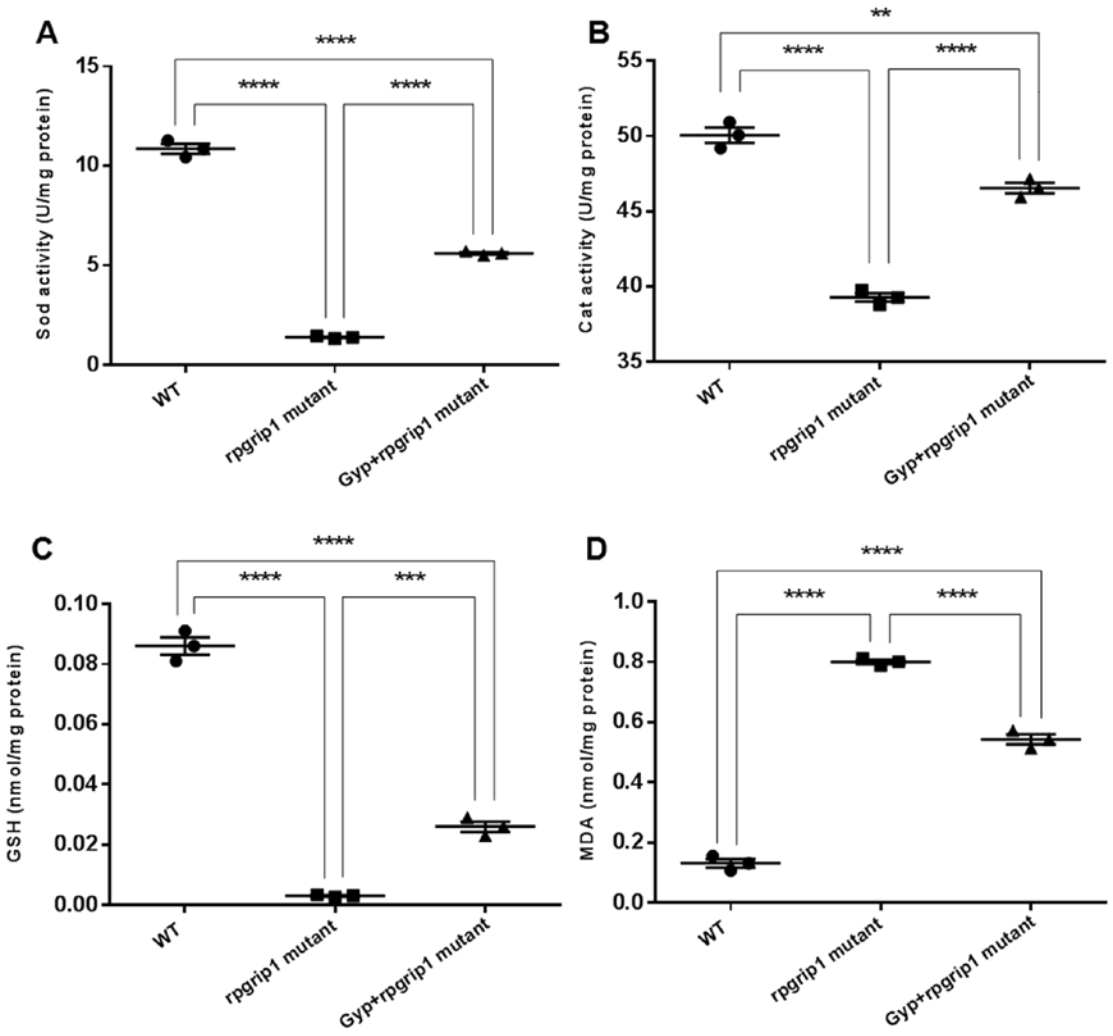

Figure 5. Gyp treatment significantly increased SOD (A) and catalase (B) activities and GSH level (C), decreased MDA level (D) in eye samples of wildtype (WT), untreated (UT) or Gyp-treated *rpgrip1* mutant zebrafish at 1 mpf. All data were analysed by one-way ANOVA followed by appropriate post hoc test (Bonferroni) and presented as mean ± SEM. $^{**}p < 0.01$, $^{***}p < 0.001$, $^{****}p < 0.0001$.

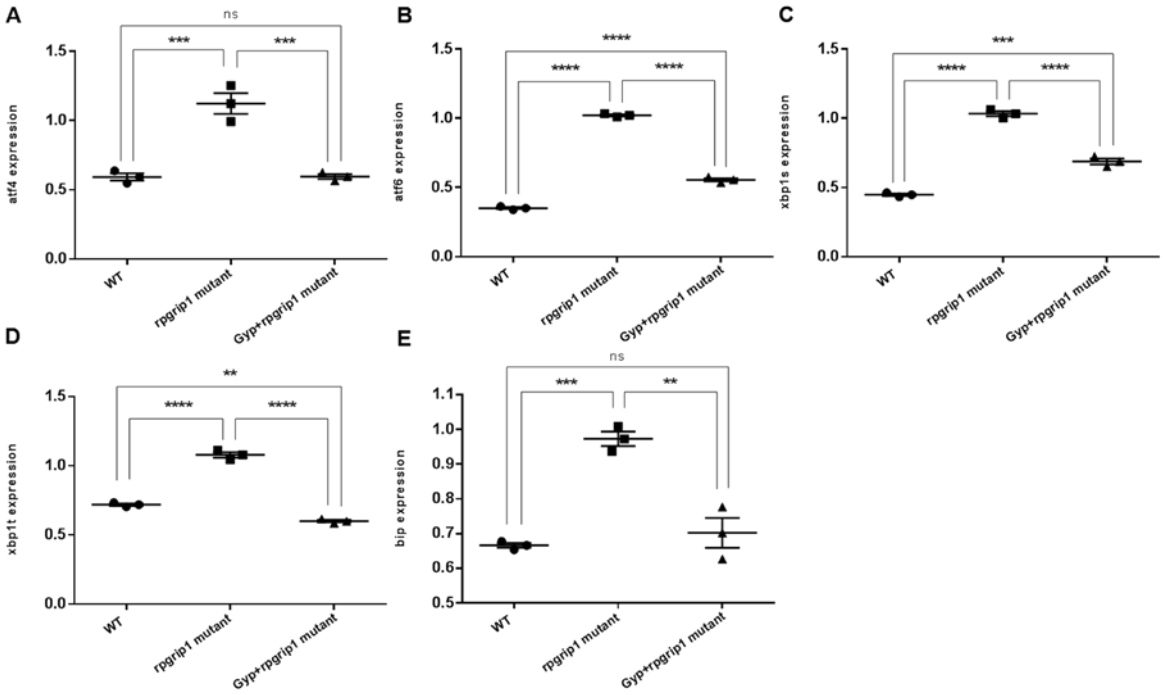

Figure 6. Expression of endoplasmic reticulum (ER) stress-related genes, *atf4* (A), *atf6* (B), *xbp1s* (C), *xbp1t* (D) and *bip* (E) in eye samples of wildtype (WT), untreated (UT) or Gyp-treated *rpgrip1* mutant zebrafish at 1 mpf was measured by qRT-PCR. All data were analysed using one-way ANOVA followed by appropriate post hoc test (Bonferroni) and presented as mean ± SEM. ns, no significance. $^{**}p < 0.01$, $^{***}p < 0.001$ and $^{****}P < 0.0001$.

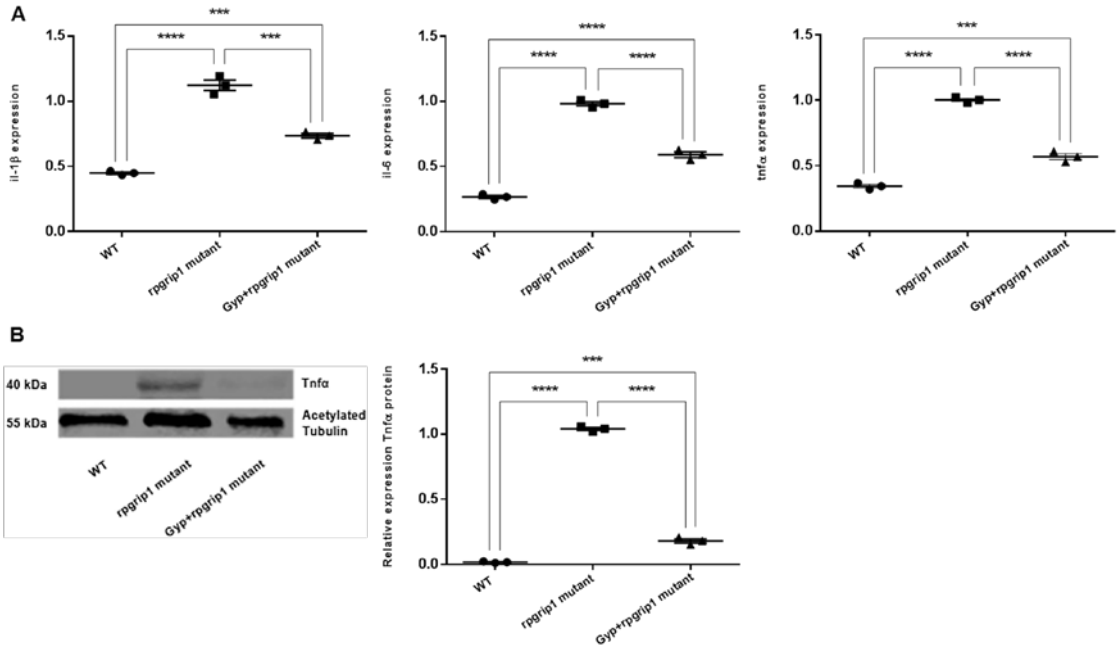

Figure 7. Gyp inhibited inflammation in *rpgrip1* mutant zebrafish eyes. (A) Expression of *il-1β*, *il-6* and *tnf-α* in eye samples of wildtype, untreated (UT) or Gyp-treated *rpgrip1* zebrafish at 1 mpf examined by qRT-PCR. (B) Protein level of Tnf-α in eye samples of wildtype, untreated (UT) or Gyp-treated *rpgrip1* mutant zebrafish detected by Western blotting. Quantification of Tnf-α level by normalization of Tnf-α intensity to the intensity of acetylated Tubulin. All data were analysed using one-way ANOVA followed by appropriate post hoc test (Bonferroni) and presented as mean ± SEM. ***$p < 0.001$, ****$P < 0.0001$.